Control of an Underactuated Self-Balancing Robotic Platform with Variable Payloads and Dynamic Uncertainties for Human–Robot Interaction

Ángel Muñoz Rocha
Graduate School of Integrated Design Engineering
Keio University
Yokohama, Japan
angelmr@keio.jp

Toshiyuki Murakami
Department of System Design Engineering
Keio University
Yokohama, Japan
mura@sd.keio.ac.jp

Abstract—This paper presents an adaptive control framework for self-balancing wheeled robots that simultaneously handles variable payloads and external disturbances during human-robot collaboration. The approach integrates Nonlinear Model Predictive Control (NMPC) with disturbance observers to achieve real-time adaptation without dedicated payload sensors. A Disturbance Observer (DOB) estimates external forces while Reaction Disturbance Observers (RDOB) infer payload mass and center-of-gravity from actuator reaction forces. These estimates continuously update the NMPC internal model, enabling seamless adaptation during manipulation tasks. A prediction error-based collision detection mechanism and supervisory Finite State Machine enhance safety during physical interaction. Simulation results with payloads up to 10 kg demonstrate stable balancing, accurate tracking, effective disturbance rejection, and real-time computational feasibility. The framework advances self-balancing robot control by unifying predictive control with observer-based adaptation for variable payload scenarios.

Index Terms—Self-balancing robot, nonlinear model predictive control, disturbance observer, variable payload, human-robot interaction, collision detection

I. INTRODUCTION

Self-balancing wheeled robots offer significant advantages in maneuverability, energy efficiency, and compactness compared to statically stable platforms. However, their inherently unstable dynamics and underactuated nature present fundamental control challenges, particularly during payload manipulation tasks in human-shared environments. When transporting objects with unknown or time-varying mass and inertial properties, continuous shifts in the system center of gravity significantly alter platform dynamics, requiring adaptive control strategies.

Model Predictive Control has emerged as an effective framework for stabilizing wheeled inverted pendulum systems due to its ability to handle constraints and predict future behavior [1], [2]. However, most implementations assume fixed parameters or discrete payload changes [3], limiting applicability during continuous manipulation. Disturbance observers have proven effective for parameter estimation and external force compensation [4], [5], yet their integration with NMPC for real-time model adaptation remains underexplored.

This paper addresses these limitations by proposing an integrated control architecture that combines NMPC with multiple disturbance observers for seamless adaptation to variable payloads. The main contributions are:

- Integration of DOB and RDOB techniques with NMPC to enable continuous adaptation to payload variations without dedicated sensors
- Real-time estimation of payload mass and center-of-gravity using reaction force measurements
- Prediction error-based collision detection compatible with varying payload conditions
- Validation demonstrating stable operation under simultaneous payload changes, motion commands, and external disturbances

The remainder of this paper is organized as follows. Section II describes the system modeling approach. Section III presents the control architecture including NMPC formulation, disturbance observers, and supervisory logic. Section IV reports simulation results, and Section V concludes the paper.

II. SYSTEM MODELING

A. Robot Description

The Two-Wheeled Forklift Robot (TWFR) consists of a differential-drive mobile base with a vertically actuated fork mechanism (Fig. 1). The platform transports loads using a prismatic actuator that extends and retracts a fork-like end effector connected via a revolute joint. Sensing is limited to wheel encoders, linear actuator position, fork joint angle, and IMU pitch measurement.

B. Simplified Dynamic Model

To enable real-time optimal control, the multibody structure is reduced to an equivalent planar rigid body characterized by total mass M, global center of gravity (x_G, z_G), and equivalent rotational inertia I_{eq}. These parameters vary as functions of payload mass, position, and lift displacement.
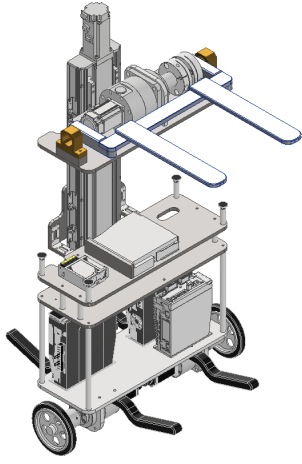
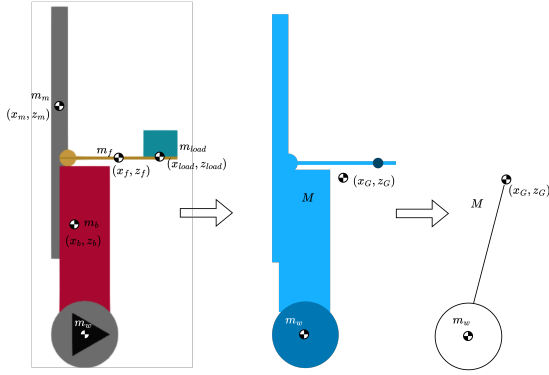Figure 1. Two-Wheeled Forklift Robot (TWFR) CAD model.

Figure 2. Simplified planar rigid body model of the TWFR showing equivalent parameters: total mass M, center of gravity position (x_G, z_G), and equivalent inertia I_{eq}.

The equivalent mass and center of gravity for $N = 4$ rigid components are:

$$M = \sum_{i=1}^{4} m_i, \quad x_G = \frac{1}{M}\sum_{i=1}^{4} m_i x_i, \quad z_G = \frac{1}{M}\sum_{i=1}^{4} m_i z_i$$

(1)

The equivalent rotational inertia using the parallel-axis theorem is:

$$I_{\mathrm{eq}} = \sum_{i=1}^{4} \left(I_{y,i} + m_i \left((x_i - x_G)^2 + (z_i - z_G)^2 \right) \right)$$

(2)

The simplified dynamics are described using generalized coordinates $q_s = [q_x \ \theta_p]^T$, where q_x is the horizontal wheel position and θ_p is the pitch angle. Applying Euler-Lagrange equations yields:

$$M_s(q_s)\ddot{q}_s + h_s(q_s, \dot{q}_s) = \boldsymbol{\tau}_s$$

(3)

where $M_s(q_s) \in \mathbb{R}^{2 \times 2}$ is the configuration-dependent inertia matrix, h_s contains Coriolis, centrifugal, and gravitational terms, and $\boldsymbol{\tau}_s$ represents generalized forces from wheel torques.

The state-space representation used for control is:

$$x_s = [q_x \ \theta_p \ \dot{q}_x \ \dot{\theta}_p]^T$$

(4)

III. CONTROL ARCHITECTURE

A. Nonlinear Model Predictive Control

The NMPC simultaneously regulates the longitudinal velocity and stabilizes the pitch angle while explicitly enforcing physical constraints. The continuous-time optimal control problem is formulated as:

$$\min_{x(\cdot), u(\cdot)} \quad \int_0^T \ell(x(t), u(t))\, \mathrm{d}t + M(x(T))$$
$$\text{subject to} \quad \dot{x}(t) = f(x(t), u(t)),$$
$$x(0) = \bar{x}_0,$$
$$g(x(t), u(t)) \leq 0.$$

(5)

The stage cost adopts a nonlinear least-squares formulation with state weighting

$$W_x = \mathrm{diag}(10^{-9}, 10^1, 10^2, 10^3),$$

(6)

which strongly prioritizes pitch stabilization. The control input is weighted using $W_u = 10^{-1} I_2$.

The NMPC is implemented using *acados* and solved via Real-Time Iteration (RTI) Sequential Quadratic Programming. The prediction horizon consists of $N = 40$ discretization steps over $T = 1$ s, corresponding to a sampling time of 25 ms. Box constraints limit the wheel torques to ± 10 Nm and the pitch angle to $\pm 45°$.

B. Disturbance Observers

1) Fork Disturbance Observer (FDOB): The FDOB estimates lumped disturbances acting on the fork joint, including dynamic coupling effects, parametric uncertainties, and external torques. Assuming a nominal inertia parameter m_{n44}, the fork dynamics are expressed as:

$$m_{n44}\ddot{\theta}_a = n_a \tau_a - \tilde{\tau}_a^{\mathrm{dist}}.$$

(7)

The disturbance is estimated using pseudo-differentiation:

$$\hat{\tau}_a^{\mathrm{dist}} = \frac{g_a}{s + g_a}\left(n_a \tau_a + g_a m_{n44}\dot{\theta}_a \right) - g_a m_{n44}\dot{\theta}_a,$$

(8)

where g_a denotes the observer bandwidth. The estimated disturbance is fed forward to augment a PD controller:

$$\tau_a = K_{pa}(\theta_a^{\mathrm{cmd}} - \theta_a) + K_{da}(\dot{\theta}_a^{\mathrm{cmd}} - \dot{\theta}_a) + \hat{\tau}_a^{\mathrm{dist}}.$$

(9)

2) Fork Reaction Torque Observer (FRTOB): The FRTOB isolates the payload-induced reaction torque from the total disturbance estimate. By excluding gravity and friction effects, the reaction torque is obtained as:

$$\hat{\tau}_a^{\mathrm{reac}} = \frac{g_r}{s + g_r}\left(n_a \tau_a + g_r m_{n44}\dot{\theta}_a - g_4 - \tilde{\tau}_a^{\mathrm{fric}} \right) - g_r m_{n44}\dot{\theta}_a,$$

(10)

where g_r is the observer bandwidth. Analogous observers (LDOB/LRFOB) are employed to estimate lift reaction forces.
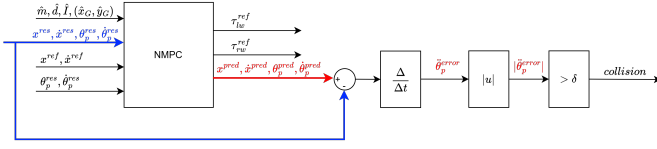
Figure 3. Control architecture for collision handling.

C. Payload Parameter Estimation

The payload mass is estimated from the lift reaction force when the actuator is active:

$$\hat{m}_{\text{lift}} = \frac{\hat{f}_m^{\text{reac}}}{g \cos(\theta_p)}. \tag{11}$$

The horizontal distance between the fork joint and the payload center of mass is estimated from the arm reaction torque:

$$\hat{d} = \frac{\hat{\tau}_a^{\text{reac}}}{g \cos(\theta_a + \theta_p)\,\hat{m}}. \tag{12}$$

These estimates are used to update the equivalent parameters $(M, x_G, z_G, I_{\text{eq}})$ of the internal NMPC model, enabling continuous adaptation to changing payload conditions.

D. Collision Detection

Collision detection exploits the predictive capability of the NMPC. The prediction error is defined as:

$$e_k = x_k - \hat{x}_{k|k-1}, \tag{13}$$

where $\hat{x}_{k|k-1}$ denotes the one-step-ahead state prediction. The time derivative of the absolute prediction error,

$$\dot{e}_k = \frac{\mathrm{d}}{\mathrm{d}t}\left(|e_k|\right), \tag{14}$$

emphasizes abrupt deviations from nominal behavior. A collision is detected when:

$$|\dot{e}_{\dot{\theta}_p,k}| > \delta_{\text{coll}}. \tag{15}$$

In self-balancing systems, the pitch-rate prediction error is particularly sensitive to external contacts.

E. Finite State Machine

A supervisory finite state machine (FSM) coordinates the operational modes (*Idle*, *Moving*, *Loading*, and *Collision*) based on boolean inputs (*Start*, *Move*, *Load*, *Collision*). During the *Loading* state, disturbance signals are ignored to ensure safe payload handling. Upon collision detection, the robot executes a backward motion and subsequently stops (Fig. 4).

IV. SIMULATION RESULTS

A. Simulation Scenario

The control architecture is validated in a challenging scenario combining sudden payload application, commanded motion, and external collision. At $t \approx 2$ s, a 10 kg payload is applied while the operator commands longitudinal motion. An impulsive collision disturbance is introduced at $t \approx 4$ s.
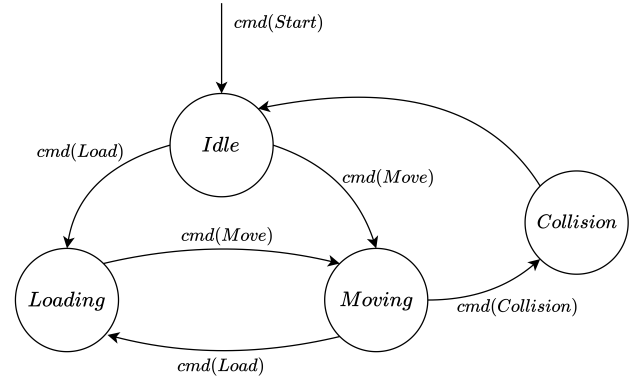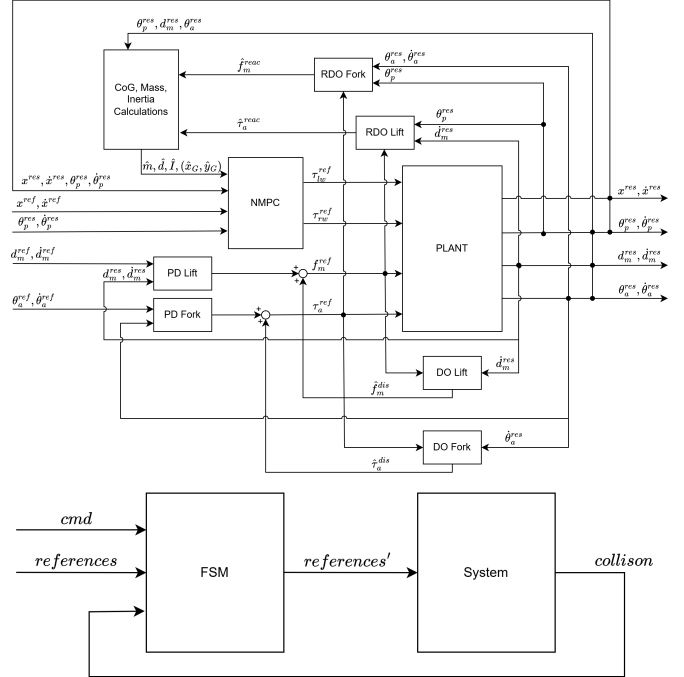

Figure 4. Finite state machine.

Figure 5. Global control architecture of the system.

B. Performance Results

Fig. 6 shows the longitudinal velocity profile. Despite abrupt dynamic changes and collision, the NMPC maintains bounded velocity and smoothly rejects disturbances, demonstrating robust stabilization.

Fig. 7 illustrates mass estimation. Following payload application, the estimator rapidly converges to the true value with well-damped transient response, confirming effectiveness under quasi-static conditions.

Fig. 8 shows the estimated horizontal distance of the payload center of mass. The estimate adapts consistently with the applied load, validating the reaction-based geometric estimation.

Fig. 9 reports the prediction error derivative. Peaks correspond to payload application and collision instants, providing
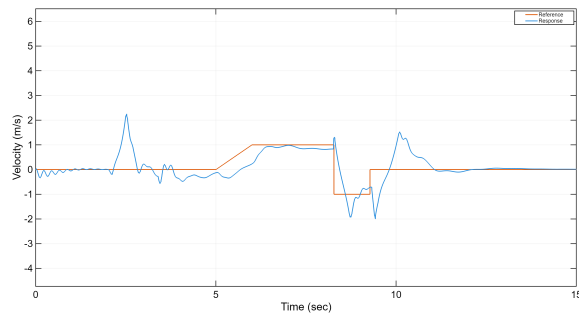
Figure 6. Longitudinal velocity during disturbance event showing stable tracking and disturbance rejection.
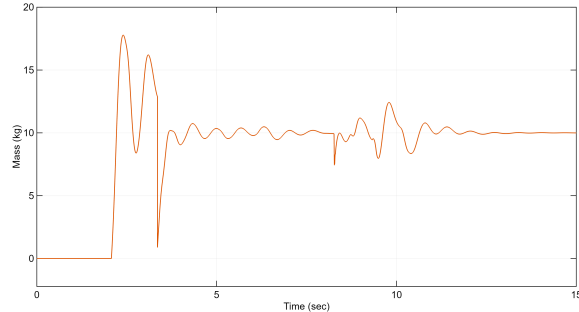

Figure 7. Payload mass estimation showing rapid convergence after load application.
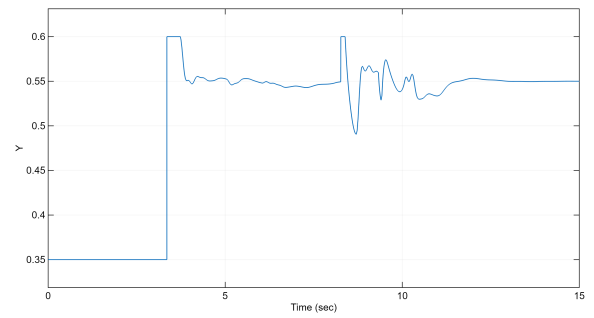

Figure 8. Distance estimation of payload center of mass from fork joint axis.

Figure 9. Absolute value of prediction error derivative highlighting disturbance events.

clear signals for interaction detection despite varying system dynamics.

Fig. 10 demonstrates computational feasibility. CPU time remains bounded throughout the simulation, confirming real-time compatibility of the NMPC configuration with RTI scheme and solver settings.

C. Discussion

The results demonstrate that integrating disturbance observers with NMPC enables seamless adaptation to variable payloads. The observers provide accurate real-time parameter estimates without dedicated sensors, while the NMPC maintains stability and tracking performance. The prediction error-based collision detection successfully identifies external interactions despite payload-induced dynamic changes. The system remains computationally efficient, supporting embedded implementation.

V. CONCLUSION

This paper presented an adaptive control framework for self-balancing wheeled robots with variable payloads. By integrating Nonlinear Model Predictive Control with Disturbance and Reaction Disturbance Observers, the approach achieves continuous adaptation to payload changes without physical sensors. Real-time estimation of payload mass and center-of-gravity enables online updating of the NMPC internal model, maintaining stable balancing and accurate tracking under dynamic uncertainties. The prediction error-based collision detection mechanism provides reliable interaction awareness

compatible with varying payloads. Simulation results validate the framework under combined payload changes, motion commands, and external collisions, demonstrating stable operation and real-time computational feasibility.

Future work includes experimental validation on the physical platform, extension to 3D motion and terrain variations, and integration with autonomous navigation capabilities for human-robot collaborative logistics applications.

REFERENCES

[1] A. Mills, A. Wills, and B. Ninness, "Nonlinear model predictive control of an inverted pendulum," in *Proceedings of the 2009 American Control Conference*. IEEE, 2009, pp. 2335–2340.

[2] A. Mishra and K. Bansal, "Control of two-wheel self-balancing robot: Lqr and mpc performance analysis," in *Proceedings of the 2024 IEEE International Students' Conference on Electrical, Electronics and Computer Science (SCEECS)*. IEEE, 2024, pp. 1–6.

[3] M. Önkol and C. Kasnakoğlu, "Adaptive model predictive control of a two-wheeled robot manipulator with varying mass," *Measurement and Control*, vol. 51, no. 1–2, pp. 38–56, 2018.

[4] H. Yajima, K. Ishizaki, Y. Miyata, M. Nawa, N. Kato, and T. Murakami, "Posture stabilization control compensating variation of body center of gravity in underactuated system," in *Proceedings of the 2023 IEEE International Conference on Mechatronics (ICM)*. IEEE, 2023, pp. 1–6.

[5] H. Kanazawa, K. Ishizaki, Y. Miyata, M. Nawa, N. Kato, and T. Murakami, "Model-based pitch angle compensation for center of gravity variation in underactuated system with an arm," in *Proceedings of the 2023 IEEE International Symposium on Industrial Electronics (ISIE)*. IEEE, 2023, pp. 1–6.
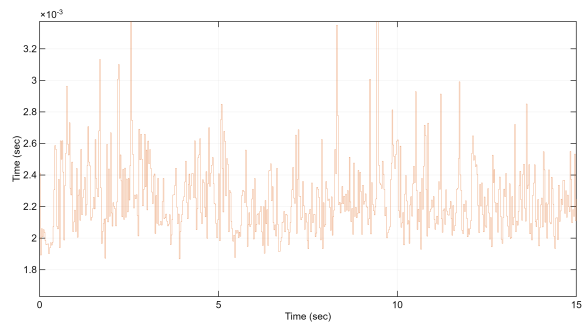
Figure 10. CPU time per control iteration showing real-time feasibility.